ELSEVIER

Journal of Hazardous Materials B92 (2002) 301–314

Journal of Hazardous Materials

www.elsevier.com/locate/jhazmat

# Oxidative pyrolysis of organic ion exchange resins in the presence of metal oxide catalysts

Ruey-Shin Juang*, Tsye-Shing Lee

*Department of Chemical Engineering, Yuan Ze University, Chung-Li 320, Taiwan, ROC*

Received 20 November 2001; received in revised form 24 January 2002; accepted 26 January 2002

**Abstract**

Pretreatment of the organic ion exchange resins by oxidative pyrolysis is effective for volume reduction before vitrification. In this work, pyrolysis of two nuclear-grade resins, Purolite NRW100 (cationic) and NRW400 (anionic), was examined using a laboratory-scale theromgravimetric analyzer (TGA) in air. It was shown that the cationic resin was harder to degrade and was less volatile compared to anionic resin. Off-gas data revealed the presence of $SO_2$, $CO_2$, CO, and $H_2O$ during oxidative pyrolysis of cationic resin from 30 to 800 °C. Trimethylamine, $CO_2$, CO, and ethyl formate were found in the case of anionic resin. In addition, oxidative pyrolysis of the mixed resins (50/50 wt.%) showed the existence of the gases nearly at the temperatures where the gases would evolve if the results of two different resins were superimposed. Several metal salts including $CuSO_4 \cdot 5H_2O$, CuO, and $FeSO_4 \cdot 7H_2O$, as well as the ions $Cu^{2+}$ pre-loaded on the resins had a catalytic effect on the oxidative pyrolysis of cationic resins, in which the decomposition of functional groups and polymer matrices was enhanced. Such catalytic effect was highlighted by a large decrease in activation energy calculated according to a degradation mechanism involving four consecutive reactions. 

*Keywords:* Oxidative pyrolysis; Organic ion exchange resins; Thermogravimetric analysis; Catalytic effect; Metal oxides; Kinetics

## 1. Introduction

For treatment of wastes, especially radioactive, vitrification has been recognized as a promising technology via volume reduction. It is preferred to common cementation since

* Corresponding author. Tel.: +886-3-4638800x555; fax: +886-3-4559373.
*E-mail address:* cejuang@ce.yzu.edu.tw (R.-S. Juang).

0304-3894/02/$ – see front matter 
PII: S0304-3894(02)00025-0

glass generally provides a more stable waste form [1]. A significant fraction of radioactive wastes is organic ion exchange resins. During vitrification of the spent resins, carbon and other remaining residues (e.g. sulfates) may harm the performance of cold crucible melter or the stability of the final glass product [2]. The remaining ash or residues from thermal treatment can be entrained by the off-gas flowing into the off-gas treatment system, and would cause significant heavy loads. Hence, it is important to first reduce the amount of such wastes entering into the melter. This can be accomplished via pyrolysis pretreatment, a thermal decomposition process that the final products are gases, liquids (tar), and solid residues (char). Such pretreatment helps further ease glass formulation restriction providing a larger glass selection base, and hence provide more economical possibilities [1].

Pyrolysis is applied with oxidation processes to further reduce the quantity of residue. In this regard, the spent resins can often be treated by one of the following combinations, pyrolysis–oxidation–ash vitrification and oxidative pyrolysis–ash vitrification [2]. They have differences in the off-gas and the ash quality and quantity being vitrified. A large quantity of off-gases likely arises in the former combination during pyrolysis and a proper off-gas treatment is required. The latter combination minimizes the build-up of potentially explosive reactants in the post-combustion chamber following thermal treatment, thereby being more economically feasible for this purpose [2].

Many fundamental and practical studies on resin pyrolysis have been made on either the laboratory- or pilot-scale [2–10]. Most of them focused on examining what amount of wastes is being reduced and the constituents of the off-gas. In general, the quality and quantity of ashes and the levels of off-gas during pyrolysis are significantly affected by the degree of cross-linking of the resins [3,4] and the environments of air or nitrogen gas [2,5–8]. For radioactive wastes, however, lowering the pyrolysis temperature becomes a major concern because it can prevent the radionuclides such as Cs-137 and Cs-134 from escaping to the off-gas stream [5,11]. The introduction of chlorine gas as an oxidant and of metal compounds as catalysts can fulfil this requirement [3,9,10]. The latter way appears to be most promising because the metals can be cyclically used in their oxide forms.

Matsuda et al. [9] examined the effect of metal impurities $Pd^{2+}$, $Cu^{2+}$, $Fe^{2+}$, $Fe^{3+}$, $Co^{2+}$, and $Ni^{2+}$, which were originally exchanged by the resins, on resin pyrolysis. The metals generally showed catalytic effects where they combined with sulfur present in functional sulfonic acid groups during thermal treatment in $N_2$ to give metal sulfides. The sulfides were then oxidized to metal oxides. Kinoshita et al. [10] pyrolyzed the cationic resins with sulfonic acid groups and the anionic resins with $–N(CH_3)_3OH$ groups in air in a fluidized bed incinerator. They also concluded that CuO is an effective catalyst.

Little attention has been paid to examining the kinetics of oxidative pyrolysis and to quantitatively clarifying the role of metal catalysts such as which decomposition step was catalyzed. In this work, route experiments were first performed in air, with and without CuO, $CuSO_4$, and $FeSO_4$, to validating the existing information by comparing the pyrolysis behavior of the two nuclear-grade resins with literature results. Studies were also made for the resins pre-loaded with metal ions. A model was proposed to describe the kinetics of the overall pyrolysis process, and the kinetic parameters were calculated using the 4th-order Runge–Kutta numerical algorithm.

## 2. Experimental

### 2.1. Resins

Nuclear-grade Purolite NRW100 (a cationic resin with sulfonic acid—$SO_3^-$ group) and NRW400 (an anionic resin with trimethylammonium—$N(CH_3)_3^+$ group) resins were used in this work, which are now used in Taiwan nuclear power plants. Physical and chemical properties of the resins are provided in Table 1. The average diameter of resin beads was roughly 0.55 mm. The density is nominally 1.2 and 1.06 g/cm$^3$ for cationic and anionic resins, respectively. The water content is 50–55% and 48–54%, respectively. Water in the beads is held in equilibrium within the hydration zone of the charged exchange sites.

### 2.2. Apparatus

A laboratory-scale theromgravimetric analyzer (TGA; Cahn TG171, USA) that is capable of pyrolyzing samples up to 1700 °C was used. The microbalance has a resolution down to 1 μg, and the weight capacity is 100 g with a 1,000,000–1 dynamic range. A chromel–alumel thermocouple is used to measure the temperature and is attached to the platinum sample crucible.

The compositions of the degraded residue were analyzed by X-ray diffraction (XRD; JEOL, Model JSM-TS330, Japan) in some cases. The off-gas was continuously analyzed using TGA (Netzsch, Model TG209, Germany) connected by Fourier transform infrared (FT-IR) spectrophotometer (Bruker, Model Vector 22, Germany). This instrument could scan the levels of gases such as CO, $CO_2$, $SO_2$, $SO_3$, NO, $NO_2$, $H_2S$, etc. Each experiment was duplicated to examine repeatability and reliability.

### 2.3. Experimental procedures

For the route TGA tests, the resins with original particle size were used to simulate the actual pyrolysis process without pre-drying. A sample of, approximately 1 g was heated at a

Table 1
Physical and chemical properties of Purolite NRW100 and NRW400

| Properties | Purolite NRW100 | Purolite NRW400 |
|---|---|---|
| Shape | Spherical bead | Spherical bead |
| Matrix | Polystyrene DVB | Polystyrene DVB |
| Degree of cross-linking | Not available | Not available |
| Functional group | Sulfonic acid ($SO_3^-$) | Trimethylammonium ($N(CH_3)_3^+$) |
| Ionic form | $H^+$ (>99.9%) | $OH^-$ (>95%), $CO_3^{2-}$ (<5%) |
| Exchange capacity (eq./l) | 1.8 | 1.0 |
| Moisture content (%) | 50–55 | 48–54 |
| Particle size (mm) | 0.425–1.2 | 0.425–1.2 |
| Specific gravity | 1.20 | 1.06 |
| Temperature limit (°C) | 120 | 60 |
| pH limit | None | None |

rate of 3 °C/min at 20 $cm^3$/s of air in the absence or presence of metal compounds. Each run was duplicated to examine the repeatability and reliability of the data. The cationic, anionic, and mixed resins (50/50 wt.%) were separately tested. Here, a low heating rate of 3 °C/min was used to minimize the temperature differences between the resins and thermocouple.

In order to prevent unwanted heat and mass transfer effects on kinetic studies, the resin was ground as powder and was sieved into 325 mesh (43 μm). The sample was pre-dried at 100 °C, and around 0.1 g of the remaining sample was heated at a rate of 5 °C/min at 20 $cm^3$/s of air. The cationic resin was tested only. The dry resins were thought to provide a better reference basis, because the variability in water content throughout the resins may make mass loss interpretations more difficult if the resin samples were wet.

## 3. Results and discussion

### *3.1. TGA results and off-gas analysis*

Many of the experimental results for cationic and anionic resins such as Amberlite IRN77 and IRN78 can be found in the literature. Although the present resins have similar active groups and properties to those used earlier, several TGA experiments were performed to compare the pyrolysis behavior. The data will provide information on evolution of resin under various test conditions. Figs. 1 and 2 show typical TGA results for oxidative pyrolysis of cationic and anionic resins. The decomposition of both resins from 30 to 800 °C can be classified into three stages, first by water evaporation, second by decomposition of active groups, and finally by combustion of polymer matrices. These findings agree with the previous results obtained under oxidizing conditions [8,9].

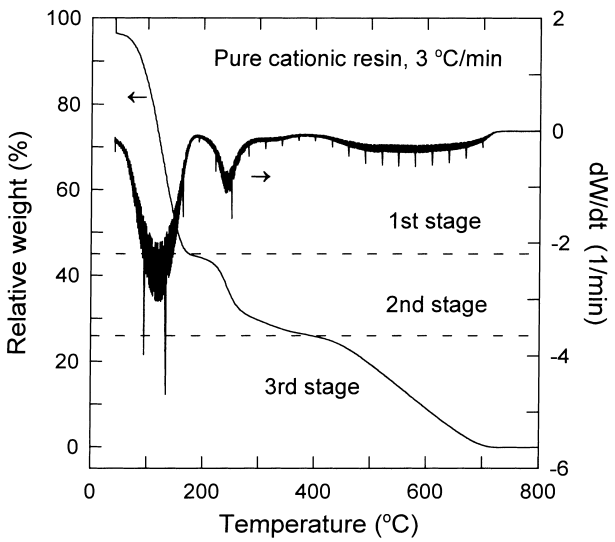


Fig. 1. TGA results for oxidative pyrolysis of pure cationic resins at 20 $cm^3$/s of air (resin particle size, 0.425–1.2 mm).

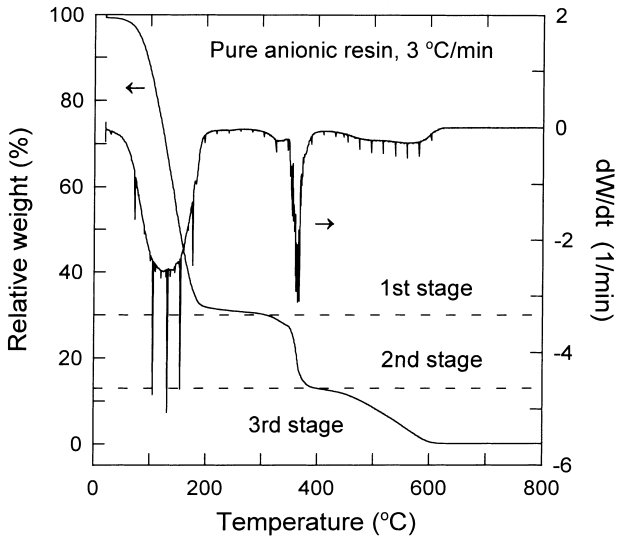


Fig. 2. TGA results for oxidative pyrolysis of pure anionic resins at 20 $cm^3$/s of air (resin particle size, 0.425–1.2 mm).

For cationic resins (Fig. 1), water vapor and trace amount of $CO_2$ are released in the 1st stage (<180 °C; off-gas data not shown). The $CO_2$ released is likely contributed by that originally dissolved in the hydrated zone or adsorbed on the resins. An initial sharp weight loss is seen. About 55% of the weight is reduced in this stage, which equals the water content of the raw resin. In the 2nd stage (180–440 °C), two breakdown regions exist in the ranges of 180–280 °C and 280–440 °C, respectively. Around 65 wt.% of the functional groups decompose in the 1st region, and the off-gases consist of $SO_2$, $CO_2$, CO, and $H_2O$. The remaining 35 wt.% likely forms sulfonyl bridges (–$SO_2$–) between polymer matrices [6]. This is supported from data that $SO_2$ is still released at higher temperatures. A very small shoulder is observed in the range 280–380 °C. Nothing seems to evolve from the resin between 380 and 440 °C. In the 3rd stage (>440 °C), the off-gases are $CO_2$, CO, and $H_2O$. The resins are fully decomposed at near 710 °C (termed as the "final" temperature hereinafter).

The present off-gas data are somewhat similar to those reported in pyrolysis of strong-acid Amberlite IRN77 cationic resins at 2 l/min of $N_2$ in a tube furnace [2]. The evolution of $SO_2$ begins at about 350 °C followed by a sharp increase resulting in two peaks at 410 and 440 °C. The $SO_2$ level sharply drops after the 2nd peak to a very low level at about 450 °C. CO starts to be detectable at near 520 °C. There are eventually two peaks for CO where one is centered at 630 °C and the other at 720 °C. Because the introduction of $O_2$ does not greatly change the temperature at which significant volatilization starts [2,8], the $SO_2$ or CO starts to release at a comparatively low temperature in this work which is partly due to the difference in degree of cross-linking of the resins [4,6]. Unfortunately, the degrees of cross-linking of the used resins are unavailable from the manufacturer or literature.

For anionic resins (Fig. 2), water vapor, trace $CO_2$, and trimethylamine are released in the 1st stage (<180 °C). About 64% of the raw resin weight is lost in this stage, beyond the

water content of the raw resin (54 wt.%). This is partly because some of the active groups loaded with $CO_3^{2-}$ begin to decompose [7]. The off-gases contain trimethylamine, $CO_2$, CO, and $H_2O$ in the 2nd stage (180–380 °C). Pyrolysis of strong-base Amberlite IRN78 anionic resin at 2 l/min of $N_2$ in a tube furnace, Chun et al. [2] also indicated that the CO starts to release during breakdown of the active groups and release of some amine gas. It was likely that methylamine is generated at 200 °C and this will be associated with a drop of nitrogen content in the residue from decomposition of the active group. In the final stage (>380 °C), the off-gases consist of $CO_2$, CO, $H_2O$, and a trace amount of ethyl formate. The final temperature of the anionic resin is 600 °C, much lower than that of the cationic resin (710 °C). It is known that anionic resin is more temperature-sensitive. When heated, Hofmann degradation may transform quaternary ammonium groups (strongly basic) into tertiary amines (weakly basic) or even destroy the active group completely [2].

In the case of the mixed resins, the FT-IR off-gas data show results that are obtained from a superposition of the gases released from the separate test of each resin (data not shown). However, the decomposition is not exactly a combination of those of pure cationic and anionic resins, as we can observe in the following section (Fig. 7). For example, the final temperature of mixed resins is around 630 °C, lying between those of both resins. This indicates that some interactions between the two residues take place [2].

### 3.2. *Effect of metal compounds on oxidative pyrolysis of the resins*

Fig. 3 shows TGA results for oxidative pyrolysis of cationic resins pre-loaded with $Cu^{2+}$ and in the presence of $CuSO_4{\cdot}5H_2O$. The final temperature in both cases (580 °C) is much lower than that of pure resins (710 °C). These metals advance the occurrence of the 3rd

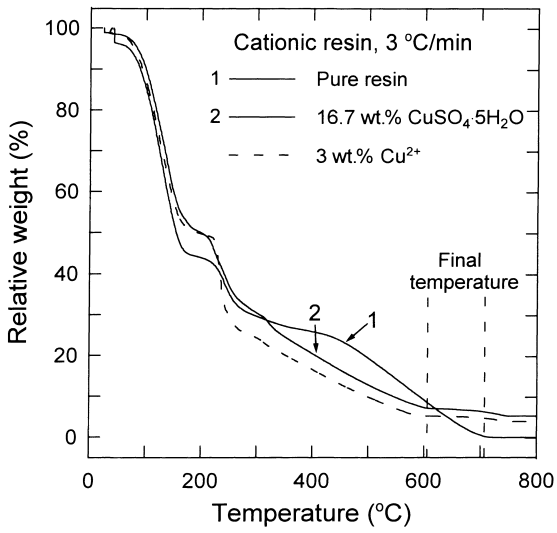


Fig. 3. TGA results for oxidative pyrolysis of cationic resins containing metal species at 20 $cm^3$/s of air (resin particle size, 0.425–1.2 mm).

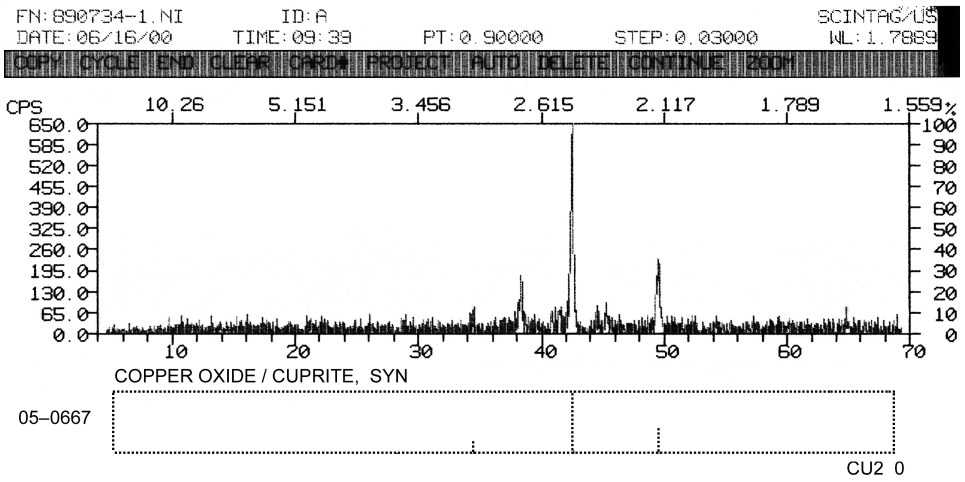


Fig. 4. XRD picture of the residue for pyrolysis of cationic resin in the presence of 6 wt.% CuO.

stage. That is, metal catalysts play an important role in the 2nd and 3rd stages, i.e. the decomposition of active groups and polymer matrices. A slight weight loss is found in the temperature range of 730–750 °C, which is likely due to decomposition of $CuSO_4{\cdot}5H_2O$ into CuO and gas $SO_3$. In general, pure $CuSO_4$ solids decompose to CuO at about 650 °C. As also indicated previously [9,10], metal ions pre-loaded by the resins combine with sulfur present in the active groups during thermal treatment in $N_2$ to give metal sulfides. The sulfides were then oxidized to the oxides. In contrast to the presence of $CuSO_4{\cdot}5H_2O$, it should be noted that the $Cu^{2+}$-loaded resin shows a more marked 2nd process combined with a correspondingly less apparent 3rd stage.

It was reported that CuO is reduced to $Cu_2O$ at a high enough temperature [12]. Here, the oven is suddenly quenched to 30 °C after the pyrolysis proceeds to 400–500 °C. XRD analysis of the residue proves the formation of the red $Cu_2O$ (Fig. 4). If the temperature is gradually lowered or the residue is contacted with air for a longer time, the black CuO forms. The catalytic role of copper impurities can be explained by the electronic effect on $O^{2-}$ of oxygen vacancies with $Cu_2O$ [13,14]. Many oxides of transition metals such as NiO, CoO, $Cr_2O_3$, and MnO have similar properties. The defect structure of $Cu_2O$ means that the oxygen excess (Cu defect) is compensated by an appropriate number of $Cu^{2+}$. The oxygen excess may enter the $Cu_2O$ lattice in which every oxygen molecule adsorbed creates four electron defects and four $Cu^{2+}$ vacancies in the interior of $Cu_2O$ crystal. These defects and vacancies lead to oxygen activation and thus an enhanced oxidation of the organic resins.

The addition of other metals such as $FeSO_4{\cdot}7H_2O$ also leads to a decrease of the final temperature (Fig. 5). The "final" temperature decreases with increasing the amount of the added CuO or $CuSO_4{\cdot}5H_2O$ to about 0.9 mmol/g. However, it reaches minimum in the presence of 5 wt.% $FeSO_4{\cdot}7H_2O$ (0.2 mmol/g), and an inverse effect is found when the amount is beyond 0.4 mmol/g. This negative effect is likely due to the formation of inert $Fe_2O_3$ at high temperatures [9,12] and, accordingly, the resin surface is fully covered.

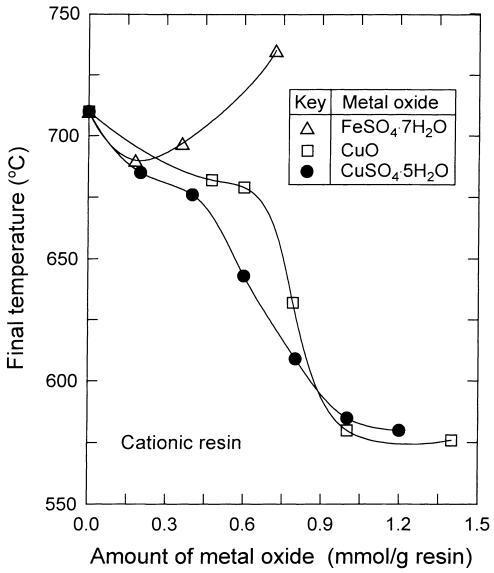


Fig. 5. Effect of the amount of added metal salts on the final pyrolysis temperature.

Fig. 6 shows TGA results for pyrolysis of anionic resin in the presence of CuO and $CuSO_4 \cdot 5H_2O$. Compared to pure resin, in both cases a more sharp weight loss is observed at temperatures very close to 100 °C (curves 2 and 3). A weight loss is found in the case of $CuSO_4 \cdot 5H_2O$ at a temperature near 250–260 °C. This is probably due to dehydration

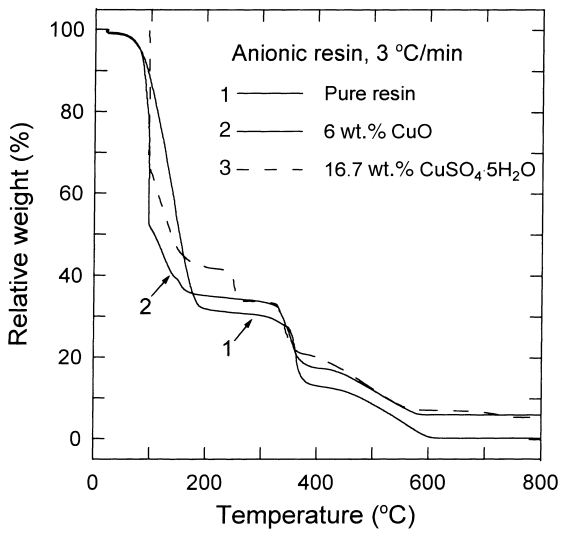


Fig. 6. TGA results for oxidative pyrolysis of anionic resins containing metal species at 20 $cm^3$/s of air (resin particle size, 0.425–1.2 mm).

of $Cu(OH)_2$, an intermediate formed in the early stages of the pyrolysis. The salt CuO also has a catalytic effect on the anionic resin, but the lowering of the final temperature is much less compared to the case of cationic resin (30 versus 130 °C). It is seen that the final temperatures of the cationic and anionic resins are equivalent (580 versus 570 °C) by the addition of metal species. The same polymer matrix and side chain can explain this behavior. The results of TGA in oxidative pyrolysis of the mixed resins also confirm this point (Fig. 7).

### *3.3. Kinetics of oxidative pyrolysis of cationic resins*

The pyrolysis kinetics of cationic resin is focused here due to its significant effect by metal oxide catalysts. From the TGA results and off-gas data, it is evident that oxidative pyrolysis of the resins is very complicated. In each stage, two or more reactions may be overlapped. As stated, the resins used for kinetic studies are ground to powders and are sieved to 43 μm to prevent unwanted heat and mass transfer effects. In addition, the sample is pre-dried at 100 °C for 24 h. Much less water is present in this case and a more overlapped 2nd and 3rd processes is expected.

Although kinetic models on thermal degradation of polymers are available [15–18], they are applicable in a rather narrower temperature range. For example, the Anderson and Freeman method [15] was applied to calculate the activation energy in the final stage of degradation of the phenol–crotonaldehyde resins [18]. Furthermore, Marcilla and Beltran [19] segmented the overall process of PVC pyrolysis into two stages and analyzed the kinetics. They demonstrated why the Friedman method [17] is not applicable when more than a single process is involved and when the data are somewhat dispersive. The overlap

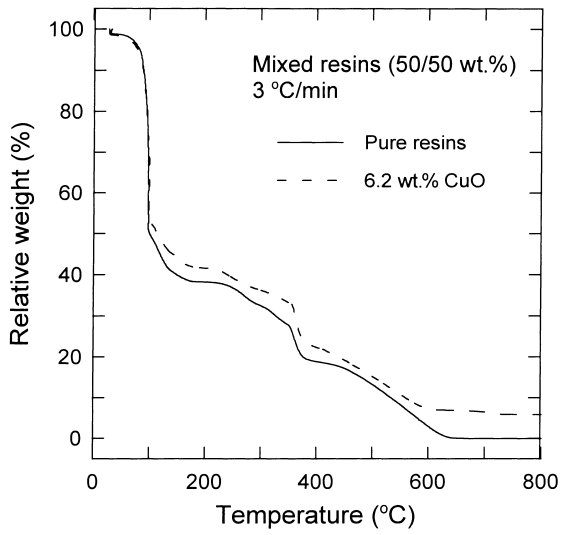


Fig. 7. TGA results for oxidative pyrolysis of the mixed resins containing metal species at 20 $cm^3$/s of air (resin particle size, 0.425–1.2 mm).

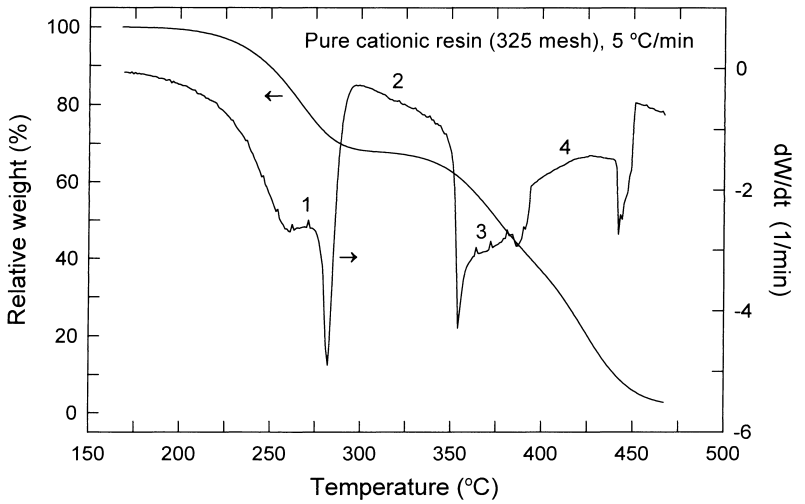


Fig. 8. TGA results for oxidative pyrolysis of pure cationic resin powders at 20 $cm^3$/s of air (resin particle size, 43 μm).

of reactions between two stages cannot be smoothly described. In practice, Marcilla and Beltran proposed different mechanisms to correlate an observed TGA curve for pyrolysis of PVC, and then to screen a best one by minimizing the model fitting error [19–21]. Their methodology is not necessarily applicable to this subject because of the different polymer matrices.

In this work, four consecutive reactions are considered according to the TGA results, in which four "peaks" exist in the rate of weight loss d$W$/d$t$ (Fig. 8) [15]:

$$R_I \xrightarrow{k_1} aG_1 + bR_A \tag{1}$$

$$bR_A \xrightarrow{k_2} cG_2 + dR_B \tag{2}$$

$$dR_B \xrightarrow{k_3} eG_3 + fR_C \tag{3}$$

$$fR_C \xrightarrow{k_4} gG_4 + hR_S \tag{4}$$

where $R_I$ is the initial dried resin, $R_S$ the residue, $R_A$, $R_B$, and $R_C$ the intermediates, $k_i$ the rate constant (1/min), $a$, $b$, $c$, $d$, $e$, $f$, $g$, and $h$ the yield coefficients (g product/g based on the initial mass), $G_1$ the gas products $SO_2$, $CO_2$, and $H_2O$, $G_2$, $G_3$, and $G_4$ are $CO_2$, $H_2O$, and CO.

The rate equations for the five species $R_I$, $R_S$, $R_A$, $R_B$, and $R_C$ are expressed as follows:

$$\frac{dR_I}{dt} = -k_{10} R_I^{n_1} \exp\left(\frac{-E_1}{RT}\right) \tag{5}$$

$$\frac{dR_A}{dt} = b\left[k_{10} R_I^{n_1} \exp\left(\frac{-E_1}{RT}\right) - k_{20} R_A^{n_2} \exp\left(\frac{-E_2}{RT}\right)\right] \tag{6}$$

$$\frac{dR_B}{dt} = d\left[k_{20}R_A^{n_2}\exp\left(\frac{-E_2}{RT}\right) - k_{30}R_B^{n_3}\exp\left(\frac{-E_3}{RT}\right)\right] \quad (7)$$

$$\frac{dR_C}{dt} = f\left[k_{30}R_B^{n_3}\exp\left(\frac{-E_3}{RT}\right) - k_{40}R_C^{n_4}\exp\left(\frac{-E_4}{RT}\right)\right] \quad (8)$$

$$\frac{dR_S}{dt} = hk_{40}R_C^{n_4}\exp\left(\frac{-E_4}{RT}\right) \quad (9)$$

where $k_{i0}$ ($i = 1$–4) is the pre-exponential factor (1/min), $n_i$ the reaction order, $R$ the universal gas constant, and $E_i$ the activation energy (kJ/mol).

The terms in the left-hand sides of Eqs. (5)–(9) correspond to the quantities of $dW/dt$. In this work, the system of rate equations is solved by the 4th-order Runge–Kutta numerical algorithm. Table 2 lists the determined parameters. The variation coefficient (VC) is also calculated to evaluate the model validity:

$$\text{VC}\ (\%) = 100 \times \sqrt{\sum \frac{[(W_{cal} - W_{exp})/W_{exp}]^2}{N - P}} \quad (10)$$

where $N$ is the number of data points and $P$ the number of parameters determined.

It is seen that the calculated results agree well with the experimental ones (Fig. 9). As shown in Table 2, the yield coefficients $b$, $d$, $f$, and $h$ nearly correspond to the points of

Table 2
Kinetic parameters obtained for oxidative pyrolysis of the dried cationic resins (particle size, 43 μm)

| Parameters | Pure resin | 22.1 wt.% $CuSO_4$ | 5.8 wt.% $FeSO_4$ |
|---|---|---|---|
| Variation coefficient (%) | 8.6 | 5.7 | 3.3 |
| Yield coefficient | | | |
| $b$ | 0.790 | 0.700 | 0.730 |
| $d$ | 0.650 | 0.665 | 0.658 |
| $f$ | 0.292 | 0.288 | 0.290 |
| $h$ | 0.014 | 0.017 | 0.016 |
| Reaction order | | | |
| $n_1$ | 1.05 | 1.05 | 1.05 |
| $n_2$ | 1.35 | 1.35 | 1.35 |
| $n_3$ | 1.47 | 1.47 | 1.47 |
| $n_4$ | 1.65 | 1.65 | 1.65 |
| Pre-exponential factor (1/min) | | | |
| $k_{10}$ | $2.30 \times 10^{10}$ | $2.45 \times 10^{10}$ | $2.35 \times 10^{10}$ |
| $k_{20}$ | $6.52 \times 10^{13}$ | $2.15 \times 10^{15}$ | $1.52 \times 10^{15}$ |
| $k_{30}$ | $7.50 \times 10^{16}$ | $9.25 \times 10^{16}$ | $8.50 \times 10^{16}$ |
| $k_{40}$ | $1.20 \times 10^{19}$ | $2.50 \times 10^{19}$ | $2.20 \times 10^{19}$ |
| Activation energy (kJ/mol) | | | |
| $E_1$ | 111.5 | 111.5 | 111.5 |
| $E_2$ | 147.0 | 141.0 | 145.0 |
| $E_3$ | 212.0 | 190.0 | 192.5 |
| $E_4$ | 252.0 | 231.0 | 229.5 |

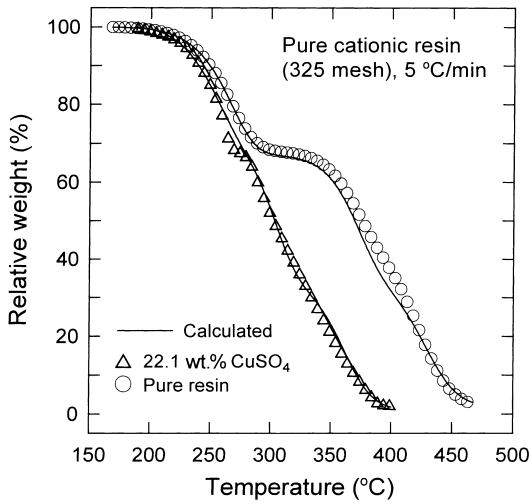


Fig. 9. Comparison of the experimental (symbols) and calculated (lines) TGA results for oxidative pyrolysis of cationic resin powders at 20 $cm^3$/s of air.

weight loss curve where a large change exists. The value of $E_2$ obtained is comparable to those of oxidation of propane (120.1 kJ/mol), ethylene (102.5 kJ/mol), and propylene (122.6 kJ/mol) in the presence of CuO catalyst [22,23]. Using similar methodology for PVC pyrolysis, Marcilla and Beltran obtained three-stage values to be $E_1 = 136.8$ kJ/mol, $E_2 = 146.5$ kJ/mol, and $E_3 = 239.1$ kJ/mol [19]. However, the activation energy in the final stage of degradation of phenol resins had a level of 102.5–115.5 kJ/mol [18]. It should be noted that $E_3$ and $E_4$ are reduced by 22 kJ/mol in the presence of $CuSO_4$ or $FeSO_4$ under the conditions studied. This justifies the findings that metal catalysts play an important role in the decomposition of active groups and polymer matrices.

### *3.4. Comments on oxidative pyrolysis of the resins*

TGA provides the weight loss phenomena as a function of temperature under various ambient conditions. Although the small-scale TGA results may not deal with other effects (e.g. turbulence, mixing, surface area exposure to gas streams, etc.) that could exist with larger-scale pyrolysis units, they should provide some fundamental understanding for the behavior of the resin which could be relevant for any scale [2]. In this work, the weight scale in TGA tests is extended to 1.0 g, which is larger than other laboratory-scale TGA dealing with a very small sample, e.g. 10 mg [8,18–21].

Previous TGA studies have shown that significant volatilization occurs during resin pyrolysis in the temperature range 300–400 °C, depending on the polymer matrices [2,6]. Matsuda et al. [7] found that optimal pyrolysis temperature for preventing resin swelling and package expansion is 300–500 °C. This meets the requirement for radioactive wastes that the pyrolysis temperature must be reduced to prevent the radionuclides from escaping to the off-gases. Although the use of metal oxides cannot fully diminish the residue within

300–500 °C, it appears to be promising due to a large volume reduction of the spent resins and the possibility of recycled use of the catalysts. Further investigations are suggested. For example, the effect of percent of each resin in the mixed sample, the presence of oxidants or other combustibles during pyrolysis, etc. should be examined.

## 4. Conclusions

Oxidative pyrolysis of two resins Purolite NRW100 and NRW400, with and without metal oxide catalysts, was studied using a small-scale TGA. Decomposition of the resins from 30 to 800 °C could be classified into three stages, water evaporation, decomposition of active groups, and combustion of polymer matrices. The cationic resin was harder to volatilize. Off-gas data showed the release of $SO_2$, $CO_2$, CO, and $H_2O$ during pyrolysis of cationic resin in air, and trimethylamine, $CO_2$, CO, and ethyl formate were found in the decomposition of anionic resin. The mixed-resin trials revealed that some interactions occurred between the two resins. The addition of metal salts such as $CuSO_4{\cdot}5H_2O$, CuO, $Cu^{2+}$-loaded, and low amounts of $FeSO_4{\cdot}7H_2O$ (<10 wt.%) enhanced the decomposition of active groups and polymer matrices, especially for cationic resin. This is due to the defect structure and electronic effect of metal oxides, leading to an activation of $O_2$ and thus an enhanced oxidation of the organic resins. The complete pyrolysis temperature of cationic and anionic resins was lowered by 130 and 30 °C, respectively, in the presence of 16.7 wt.% $CuSO_4{\cdot}5H_2O$. A degradation mechanism involving four consecutive reactions was proposed for cationic resin based on the occurrence of four "peaks" in the rate curve of weight loss. The predicted TGA results agreed well with the measured ones (variation coefficient $< 8.6\%$). The decrease in activation energies in the final two reactions, $E_3$ and $E_4$, by 22 kJ/mol due to the addition of $CuSO_4$ or $FeSO_4$ could identify the role of metal oxide catalysts.

## Acknowledgements

Support for this work by the Taiwan Electric Co. and National Science Council, ROC under Grant No. NSC89-TPC-7-155-002 is gratefully appreciated.

## References

[1] J.K. Park, H.J. Ahn, Y.S. Kirn, M.J. Song, Technical and economic assessment for vitrification of low-level radioactive waste from nuclear power plants in Korea, in: Proceedings of the Waste Management Conference, 25–29 February, Tucson, AZ, 1996.
[2] U.K. Chun, K. Choi, K.H. Yang, J.K. Park, M.J. Song, Waste minimization pretreatment via pyrolysis and oxidative pyrolysis of organic ion exchange resin, Waste Manage. 18 (1998) 183–196.
[3] B. Elvers, S. Hawkings, M. Ravenscroft, G. Schuiz, Ion exchangers, in: Ullmann's Encyclopedia of Industrial Chemistry, Vol. A14, VCH Publishers, New York, 1989, pp. 394–410.
[4] J.W. Neely, Characterization of polymer carbons derived from porous sulfonated polystyrene, Carbon 19 (1981) 27–36.
[5] S. Pettersson, G. Kemmier, Experience of resin pyrolysis, in: Waste Management 84, Vol. 2, Arizona Board of Regents, Arizona, 1984, p. 223.

[6] M. Matsuda, K. Funabashi, H. Yusa, Influence of functional sulfonic acid group on pyrolysis characteristics for cation exchange resin, J. Nucl. Sci. Technol. 24 (1987) 124–128.
[7] M. Matsuda, K. Funabashi, T. Nishi, H. Yusa, M. Kikuchi, Decomposition of ion exchange resins by pyrolysis, Nucl. Technol. 75 (1986) 187–192.
[8] M.A. Dubois, J.F. Dozol, C. Nicotra, J. Serose, C. Massiani, Pyrolysis and incineration of cationic and anionic ion exchanger resins. Identification of volatile degradation compounds, J. Anal. Appl. Pyrolysis 31 (1995) 129–140.
[9] M. Matsuda, K. Funabashi, H. Yusa, Effect of metallic impurities on oxidation reaction of ion exchange resin, J. Nucl. Sci. Technol. 23 (1986) 244–252.
[10] K. Kinoshita, M. Hirata, T. Yahata, Treatment of ion exchange resins by fluidized bed incinerator equipped with copper oxide catalyst. Fundamental studies, J. Nucl. Sci. Technol. 28 (1991) 228–238.
[11] B.D. Amiro, S.C. Sheppard, F.L. Johnston, W.G. Evenden, D.R. Harris, Burning radionuclide question: what happens to iodine, cesium and chloride in biomass fires? Sci. Total Environ. 187 (1996) 93–103.
[12] Z.G. Szabo, D. Kallo, Defect structure and electrical behavior of semiconductor oxides, in: Contact Catalysis, Vol. 1, Wiley, New York, 1976, pp. 85–124.
[13] H.J. Freund, Oxide surfaces, Faraday Discussion 114 (1999) 1–31.
[14] L. Triguero, S. de Carolis, M. Baudin, M. Wojcik, K. Hermansson, M.A. Nygren, L.G.M. Pettersson, Metal oxides: $O^{2-}$ chemistry and dynamic effects on oxide reactivity, Faraday Discussion 114 (1999) 351–362.
[15] D.A. Anderson, E.S. Freeman, The kinetics of thermal degradation of synthetic styrenated polyester, J. Appl. Polym. Sci. 1 (1959) 192–199.
[16] H.H. Horowitz, G. Metzger, A new analysis of thermogravimetric traces, Anal. Chem. 35 (1963) 1464–1468.
[17] H.L. Friedman, Kinetics of thermal degradation of char-forming plastics from thermogravimetry. Application to a phenol plastic, J. Polym. Sci. Part C 6 (1965) 183–195.
[18] M.P.R. Rao, B.S.M. Rao, C.R. Rajan, R.S. Ghadage, Thermal degradation kinetics of phenol–crotonaldehyde resins, Polym. Degrad. Stab. 61 (1998) 283–288.
[19] A. Marcilla, M. Beltran, Thermogravimetric kinetic study of poly(vinyl chloride) pyrolysis, Polym. Degrad. Stab. 48 (1995) 219–229.
[20] A. Marcilla, M. Beltran, Kinetic models for thermal decomposition of commercial PVC resins and plasticizers studied by thermogravimetric analysis, Polym. Degrad. Stab. 53 (1996) 251–260.
[21] M. Beltran, A. Marcilla, Kinetic models for thermal decomposition of PVC plastisols, Polym. Degrad. Stab. 55 (1997) 73–87.
[22] Y. Morooka, A. Ozaki, Regularity in catalytic properties of metal oxides in propylene oxidation, J. Catal. 5 (1966) 116–124.
[23] Y. Morooka, Y. Morikawa, A. Ozaki, Regularity in the catalytic properties of metal oxides in hydrocarbon oxidation, J. Catal. 7 (1967) 23–32.